International Journal of Biological Macromolecules 87 (2016) 488–497

Contents lists available at ScienceDirect

International Journal of Biological Macromolecules

journal homepage: www.elsevier.com/locate/ijbiomac

Immobilization of a novel cold active esterase onto Fe_3O_4~cellulose nano-composite enhances catalytic properties

Mohammad Asadur Rahman[a,b,1], Umma Culsum[a,b,1], Ashok Kumar[b], Haofeng Gao[a], Nan Hu[a,*]

[a] College of Biotechnology and Pharmaceutical Engineering, Nanjing Tech University, Nanjing 211800, China
[b] State Key Laboratory of Agricultural Microbiology, College of Life Science and Technology, Huazhong Agricultural University, Wuhan 430070, China

ARTICLE INFO

Article history:
Received 11 February 2016
Received in revised form 8 March 2016
Accepted 9 March 2016
Available online 11 March 2016

Keywords:
Cold active
Immobilization
Nano-composites
Salt tolerance

ABSTRACT

A novel esterase, EstH was cloned, purified and characterized from the marine bacterium *Zunongwangia* sp. The purified EstH showed optimum activity at 30 °C and pH 8.5 with ~50% of original activity at 0 °C. EstH was stable in high salt conditions (0–4.5 M NaCl). To improve the characteristics and explore the possibilities for application, a new immobilization matrix, Fe_3O_4~cellulose nano-composite, was prepared and was characterized by Fourier Transform Infrared Spectroscopy (FTIR) and Scanning Electron Microscope (SEM). Interestingly the optimal temperature of immobilized EstH elevated to 35 °C. Compared to its free form, immobilized EstH showed better temperature stability (48.5% compared to 22.40% at 50 °C after 30 min), prolonged half-life (32 h compared to 18 h), higher storage stability (~71% activity compared to ~40% after 50 days of storage), improved pH tolerance (~73% activity at pH 4 and 10), and, more importantly, reusability (~50% activity after 8 repetitive cycles of usage). Enzyme kinetics showed an increase in the V_{max} (from 35.76 to 51.14 μM/min) and K_{cat} (from 365 s^{-1} to 520 s^{-1}) after immobilization. The superior catalytic properties of immobilized EstH suggest its great potential in biotechnology and industrial processes.

© 2016 Elsevier B.V. All rights reserved.

1. Introduction

Esterases (EC 3.1.1.1) of microbial origin with good stability and activity have potential applications in food and dairy industries, detergents, pharmaceuticals, synthesis of optically pure compounds, bioremediation, perfume production and even in biomedical device production [1–4]. Esterases with some unusual characteristics such as cold active are energy saving and easy to be inactivated in synthetic reactions is useful in the production of heat sensitive materials [5–7]. On the other hand, esterases which are stable in high pH and salt conditions, can catalyze reactions in both nonaqueous and aqueous/organic media and can be utilized to degrade organic matters in saline water [8–10]. Moreover, structural modification and immobilization could contribute to the thermostability of cold adapted enzymes as compared to the free enzymes [11–14].

Immobilized enzymes can maintain the conformational change and the physiochemical properties, prevent the enzyme from being aggregated in organic media and continuous reaction processes, reduce the possibility of denaturation in the conditions of high temperature, pH and organic solvents, and also facilitate storage and maintenance compared with the free ones [15–20]. Furthermore, immobilization is very crucial for the production of fine chemicals by removing the enzyme from reaction system and control over product formation [21].

The chemical structure of immobilization support and large surface area are the important factors to achieve sufficient enzyme loading and catalytic efficiency in aqueous or organic media [22]. Organic and inorganic nanoparticles with a large surface area are proved to be excellent materials for immobilization of enzymes. Furthermore, selection of a suitable immobilization method is another important factor for the successful immobilization of an enzyme. Magnetic nanoparticles like Fe_3O_4 have been used efficiently in immobilization because of their superparamagnetism, high surface area, easy separation from the reaction mixture by applying magnetic fields as well as controlling mechanism of the orientation on the enzymes attached to the support [23–26]. Surface modification or coating of Fe_3O_4 nanoparticles with organic materials can enhance the binding efficiency of an enzyme with

* Corresponding author: College of Biotechnology and Pharmaceutical Engineering, Nanjing Tech University, Nanjing 211800, China.
E-mail addresses: nayongeb@gmail.com (M.A. Rahman), eshageb@gmail.com (U. Culsum), ashok.nadda09@gmail.com (A. Kumar), zane_gao1986@163.com (H. Gao), hunan@njtech.edu.cn (N. Hu).
[1] Authors have equal contribution to the work.

http://dx.doi.org/10.1016/j.ijbiomac.2016.03.016
0141-8130/© 2016 Elsevier B.V. All rights reserved.

the support materials either by hydrogen bonding or van der Waals interaction or electrostatic interactions. In recent studies, nanocellulose has been synthesized from various natural sources which proved to be a good template for the formation of nano-composites [27]. Nanocellulose shows a unique property to self-assemble with improved thermal stability as well as solvent stability [28]. Thus, cellulose-based nano-composites with inorganic materials like Fe_3O_4 nanoparticles can sustain relatively high temperatures, pH and extreme physiochemical conditions and provide well-defined mesostructure with metal oxide scaffolds to protect any biomolecules like protein/enzyme from denaturation [29,30]. In recent years, cellulose of different origins has been used as a supporting matrix for the formation of iron oxide and as filler for the homogeneous distribution of pre-synthesized crystalline nanostructures [29,31,32].

In the present study, a novel family VII cold active and salt tolerant esterase from *Zunongwangia* sp. was purified and immobilized onto a Fe_3O_4~cellulose nano-composite. Both Fe_3O_4 nanoparticles and nanocellulose were synthesized separately and assorted by sol-gel method to prepare a hybrid nano-composite. The purified esterase was immobilized onto this nano-composite and the improved bio-catalytic properties were studied in comparison with those of the free esterase.

2. Material and methods

2.1. Strains, vectors and chemicals

The marine bacterium *Zunongwangia* sp. and its genome have been already reported [33]. It was grown in high-salt Luria-Bertani medium (HLB) (peptone 1%, yeast extract 0.5%, NaCl 2%) at 28 °C. *Escherichia coli* strains DH5α (Takara, Japan) and BL21 (DE3) (Novagen, USA) were used as the bacterial hosts for plasmid (pGEX-6P-1, GE Healthcare, USA) amplification and heterologous expression, respectively. The enzymes used such as restriction endonucleases, DNA polymerase, and T4 DNA ligase were purchased from Takara (Kyoto, Japan) and the substrates, *p*-nitrophenyl esters: *p*-nitrophenyl acetate (C2), *p*-nitrophenyl butyrate (C4), *p*-nitrophenyl hexanoite (C6), *p*-nitrophenyl caprylate (C8), *p*-nitrophenyl laurate (C12), and *p*-nitrophenyl palmitate (C16) were purchased from Sigma-Aldrich (St. Louis, MO, USA) and Microcrystalline cellulose (MCC) was procured from Merck Schuchardt, Germany. All the other chemicals and buffers used were of high purity and analytical grade.

2.2. Gene cloning and recombinant plasmid construction

The putative esterase containing gene EstH encodes a protein (GenBank No. ADF54626.1) which was amplified using the genomic DNA of *Zunongwangia* sp. as template with the following primers EstH F: 5′ CGCGGATCCATGAAAAAAATCATACTGTTATTTGCA -3′ and EstH R: 5′- CCGCTCGAGTTATTGTTCGGTGTACTTTTTATCTAA -3′ with restriction enzyme sites of *Bam*HI and *Xho*I, (underlined) respectively. PCR was performed in a thermal cycler programmed with 95 °C for 30 s, 30 cycles of 94 °C for 30 s, 57 °C for 30 s and 72 °C for 1.40 min and a final elongation of 72 °C for 10 min. Then the PCR products were purified using 1% agarose gel using gel mini purification kit (AXYGEN, USA). Next, the vector and purified PCR products were digested with *Bam*HI and *Xho*I, and purified by gel. The digested and purified gene was cloned into the digested and purified pGEX-6P-1 vector using T4 DNA ligase and transformed into the competent *E. coli* DH5α cells, followed by incubation in solid LB medium (1% NaCl, 1% peptone, 0.5% yeast extract, 1.5% agar) supplemented with 100 μg/ml ampicillin at 37 °C overnight, and then the recombinant plasmids were extracted. Finally, the correct insert of the plasmid was confirmed by sequencing, and the recombinant plasmid of pGEX-6P-1-EstH was used for further study.

2.3. Expression and purification of EstH

The recombinant plasmid pGEX-6p-1-EstH was transformed into *E. coli* BL21 (DE3) competent cells for expression. *E. coli* BL21 (DE3) cells containing the recombinant plasmid pGEX-6P-1-EstH were grown in the liquid LB medium containing 100 μg/ml ampicillin at 37 °C overnight, followed by inoculation at 1:100 dilution into fresh LB liquid medium containing 100 μg/ml ampicillin and incubation at 37 °C till OD_{600} reached 0.6. Then 1 mM (final concentration) IPTG was added and cultured for 16 h at 18 °C and 180 rpm. Next, the cells were collected and washed twice with PBS buffer (0.8% NaCl, 0.02% KCl, 0.142% Na_2HPO_4, 0.027% KH_2PO_4; pH 7.4) by centrifugation at 8000 rpm for 10 min and resuspended in PBS buffer and then the cells were disrupted by a French press and the crude enzyme was obtained as supernatant by centrifugation at 12000 rpm for 40 min at 4 °C. Finally, glutathione-S transferase (GST)-tagged fusion esterase GST-EstH was purified according to manufacturer's instructions using Glutathione Sepharose 4B columns (GE Healthcare). 3C protease solution (10 U/μl PreScission; Pharmacia) was used to remove the GST tag and the purified protein was eluted with a moderate amount of PBS buffer (pH 7.4). The protein was quantified with Bradford reagent (Sigma, USA) using bovine serum albumin (BSA) as a standard [34] and the proteins were analyzed by 12% SDS-PAGE.

2.4. Sequence analysis

The sequence similarity was examined by Basic Local Alignment Search Tool (BLAST) program from the server at National Centre of Biotechnology, USA (http://blast.ncbi.nlm.nih.gov/Blast.cgi). Multiple sequence alignment was done by the Clustal W Method of BioEdit Sequence Alignment Editor Program. Phylogeny analysis was performed using the sequences of previously determined I-VIII family esterases/lipases [35] with MEGA 6.0 program [36].

2.5. Enzyme activity assay

One unit of esterase activity was determined by the production of 1 μmol of *p*-nitrophenol from *p*-nitrophenyl butyrate (*p*NPB, C4) in 1 min using *p*-Nitrophenol as standard. The volume of each standard reaction mixture was 200 μl consisting of 3 μl of 20 mM substrate, 2 μl of pure enzyme (2 μl of immobilized enzyme suspension) and 195 μl Tris–HCl buffer (50 mM, pH 8.5), and the reaction mixture without the addition of any enzyme was considered as standard. The reaction continued for 7 min at 30 °C for the free enzyme and 35 °C for the immobilized one with continuous shaking, followed by the separation of immobilized biocatalyst by applying magnetic field, and the absorbance of the released *p*-nitrophenyl was recorded at 405 nm using 96-well plate with Thermo Scientific Multiscan Spectrum.

2.6. Synthesis of Fe_3O_4~cellulose nano-composite

The spherical cellulose nanogel was prepared by controlled acidic hydrolysis as previously described [37] with minor modifications [38]. Nanogel was prepared by mixing 5 g of MCC in 50 ml distilled water and H_2SO_4 was as added drop by drop to a final concentration of 63.4 wt% under shaking condition. Later on, the solution was transferred into 10-fold volume of cold water, separated by centrifugation and neutralized with dd H_2O and Na_2CO_3 (2% v/v). Then, the cellulose nanogel was washed, diluted (5 wt%)

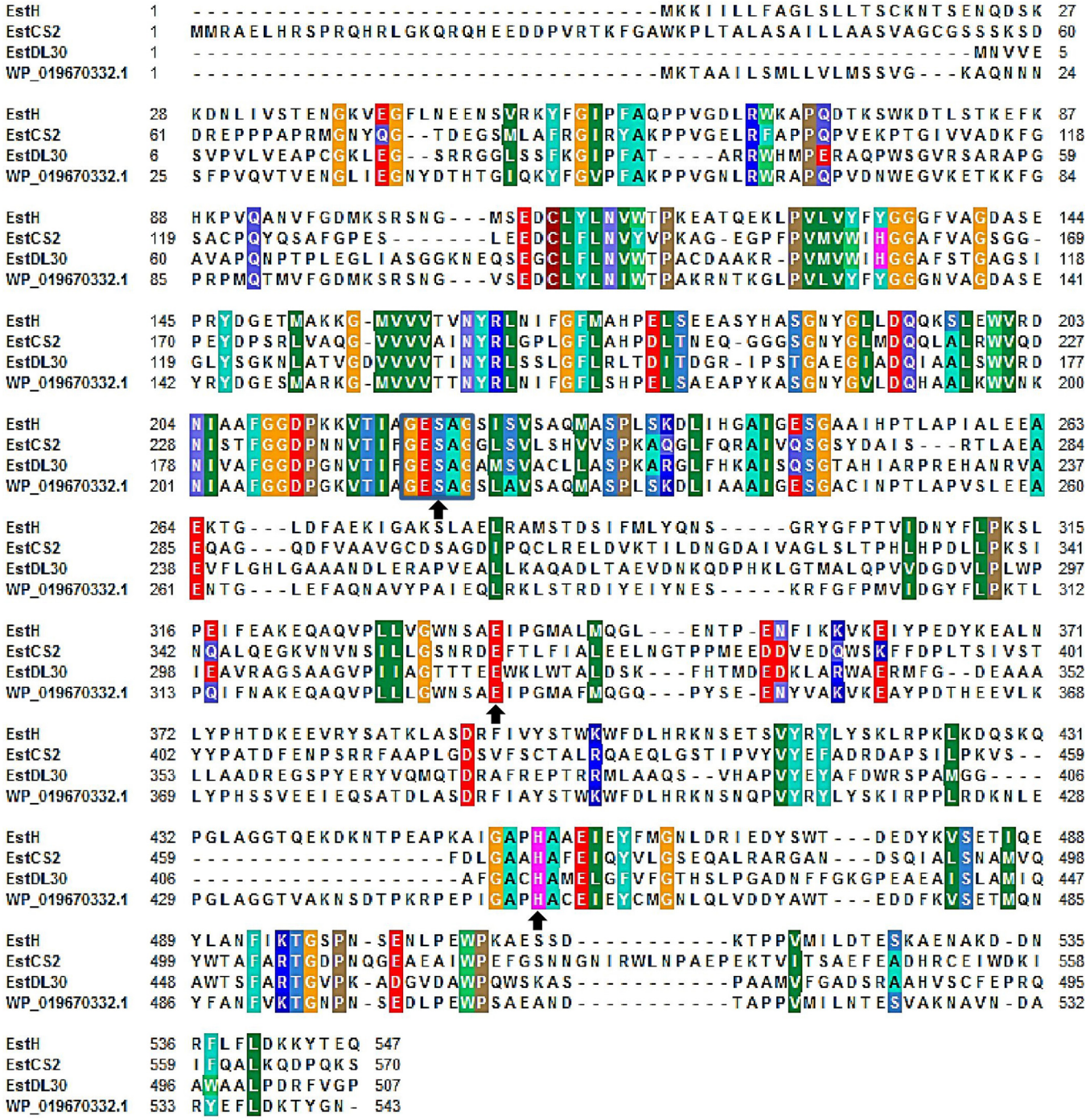

Fig. 1. Amino Acid sequence alignment. Amino acid Sequence alignment of EstH with other members of α/β hydrolase superfamily, Famly VII esterase, estDL30 and estCS2 from metagenomic library and putative carboxylesterase from *E. adriatica* (WP_019670332.1). The catalytic triads, Ser 221-Glu 3337-His 456, are indicated by a black filled arrow and the conserved motif Gly 219-X-Ser 221-X-Gly 223 is indicated by a black box.

and homogenized with a high-pressure homogenizer. After washing the absolute ethanol, acetone, hexane and distilled water, the prepared nanogel was stored in distilled water for further use.

The magnetic nanoparticles (MNPs) were synthesized using the modfied chemical co-precipitation method [39]. The iron oxide slats ($FeCl_3{\cdot}6H_2O$; 4.2 g and $FeCl_2{\cdot}4H_2O$; 2.16 g) were dissolved in 200 ml of dd H_2O in nitrogen rich environment under continuous stirring. The reaction mixture was incubated at 85 °C for 5 min and then supplemented with 40 ml of ammonia. The reaction ran for 12 h and megnetic nanoparticles were collected by megnetic separation and washed 3 times with ddH_2O. MNPs coated with nano-cellulose were synthesized by the sol–gel reaction. Firstly, Fe_3O_4 particles were washed 3 times with ethanol, and dispersed in 200 ml of ethanol. Afterward, 50 mg of MNPs were mixed with 4 ml of nanocellulose suspension in the dispersion solution and incubated at 45 °C under shaking (180 rpm) for 12 h. The nano-composites were separated from the reaction mixture and washed separately with distilled water, absolute ethanol, hexane and stored at 4 °C for further use.

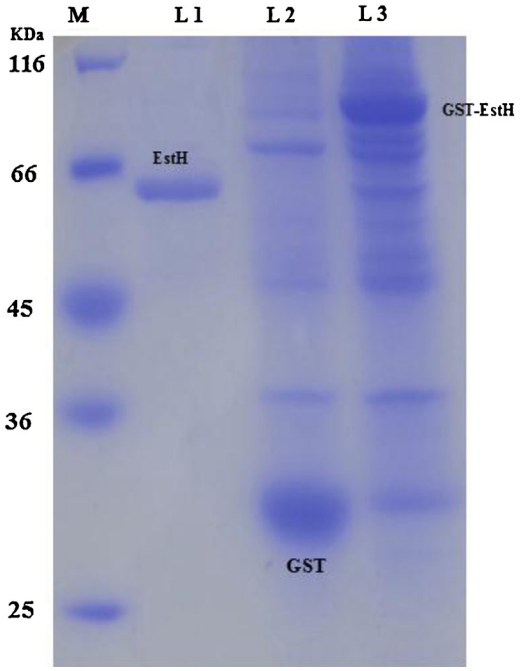

Fig. 2. SDS-PAGE analysis of purified EstH. Lane M, the standard protein molecular mass marker; Lane 1, the purified EstH from the vector pGEX-6p-1-EstH (MW 61.2 kDa); Lane 2, induced cell supernatant of pGEX-6p-1 as control; Lane 3, induced cell supernatant from the vector pGEX-6p-1-EstH.

2.7. Characterization of Fe_3O_4~cellulose nano-composite

The Fe_3O_4~ cellulose nanocomposite was studied by Fourier Transform Infrared Spectroscopy (FTIR; NEXUS 870, Thermo, Madison, USA) and Transmission Electron Microscopy (TEM; Hitachi, Tokyo, Japan). A KQ3200E ultrasonicator with the ultrasonic frequency of 40 kHz (KunShan Ultrasonic Instruments Co., Ltd. KunShan, China) was used to disperse the cellulose nanogel.

2.8. Immobilization of purified esterase onto Fe_3O_4~cellulose nano-composite

To immobilize EstH with the nanocomposites, purified EstH was mixed with the slurry of Fe_3O_4~cellulose nanocomposite at the ratio of 1:4 and incubated at 4 °C under mild shaking for 12 h. After overnight incubation, the biocatalyst mixture was centrifuged (10000 rpm) and the supernatant was removed by decantation. The nanocomposite bound esterase was washed 3 times with PBS to remove the unbound or loosely bound protein. The protein loading/immobilization yield (IY) and immobilization efficiency (IE) were determined using previously described method [40].

2.9. Comparison of hydrolytic properties of free and immobilized EstH

The substrate specificity of EstH was determined by the standard method with the different acyl chain lengths of *p*-NP esters from C2 to C16. The optimal temperature was determined by incubating the reaction mixture from 0 to 80 °C for 5 min. For thermostability assay, the enzyme was incubated in a temperature range of 30–60 °C and samples were collected every 30 min for 3 h. The residual effect was determined by standard condition. Enzyme activity without any incubation was considered as 100%. Buffer with various pH values, phosphate–citrate buffer (pH 4.0–8.0) and Tris–HCl buffer (pH 8.0–10.0) were used to determine the optimal pH. pH stability was determined by measuring the remaining activity after incubating the enzyme for 24 h at 4 °C in the same pH buffer.

The effects of various organic solvents (methanol, acetonitrile, isopropanol, ethanol, *n*-propanol, Dimethyl sulfoxide (DMSO) and ethylene glycol) and detergents (Tween-20, Tween-80, sodium dodecyl sulfate (SDS), cetyltrimethylammonium bromide (CTAB) and Triton X-100) were determined by pre-incubating both the free and immobilized EstH enzymes separately with different concentrations of organic solvents (10–40%, v/v) and detergents (5% v/v) for 40 min and 1 h respectively.

The decrease the 50% of its original activity was recorded. The reusability of immobilized EstH was measured through repetitive cycles at standard condition using *p*-nitrophenyl butyrate as substrate. After every assay, the immobilized EstH was recovered and washed three times with PBS buffer and added to a fresh reaction system to determine the enzyme activity of the next run. This step was repeated 10 times and the remaining activity was measured after each run and the activty in its initial step was determined as 100%. To evaluate the storage stability, both free and immobilized EstH forms were stored at 4 °C for 50 days and the remaining activity was measured at an interval of 5 days under stardard conditions. The half life was determined by incubating the both forms of the biocatalyst at their optimal temperature for 34 h. The hydrolytic activity was determined after each 30 min.

The effects of NaCl on the activity and stability of EstH were also tested with varying concentrations (1–4.5 M). The specific activity without NaCl was defined as 100%. Stability was determined by incubating the enzyme in pH 8.5 Tris-HCl (50 mM) buffer with different concentrations of NaCl at 4 °C for 12 h, and the relative activity was determined under the standard conditions. The specific activity after incubation with 0 M NaCl was defined as 100%. Different concentrations of *p*-nitrophenyl butyrate ranging from 1 to 80 mM were used to measure the initial rate of reaction. Michaelis–Menten constant (K_m), was determined according to Lineweaver–Burkplot, and the catalytic constant (*K*cat) was calculated according to the value of V_{max}, the molecular weight and the concentration of the purified protein using the Graphpad Prism software (Graphpad, San Diego, CA, USA).

3. Results

3.1. Gene cloning and sequence analysis of EstH

The putative esterase encoding gene, EstH was successfully cloned from *Zunongwangia* sp. with a length of 1644 bp,

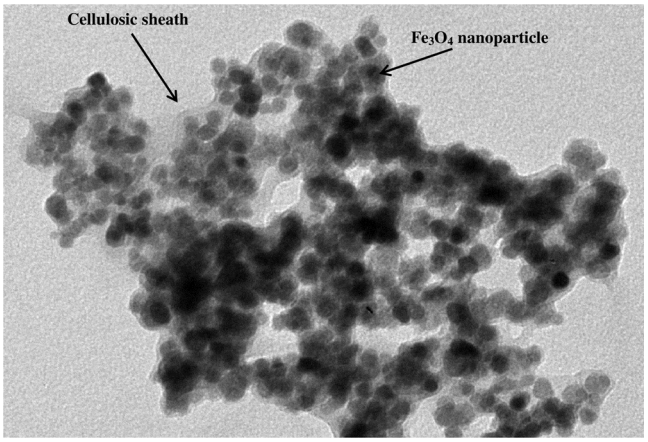

Fig. 3. TEM images of nano-composite. TEM images of Nanocellulose-Fe_3O_4 nanocomposite.

Table 1
FTIR spectra of nano-composite.

Type of chemical bond	Frequency (cm^{-1})	Possible assignment
C—H of cellulose	2850	Bond streching
O—H of cellulose	2900	Bond streching
C—H of cellulose	897	Bond vibraton and deformation
O—H of cellulose	1371	Bond vibration and deformation
CH_2 group of cellulose	1430	absorption
C=O	1060	stretching vibration
Anomeric carbon of cellulose	895	absorption
Fe—O	582–588	absorption

encoding 547amino acid residues with a calculated molecular mass of 61.2 kDa. EstH shows 65% similarity with hypothetical carboxylesterase from *Maribacter* sp. Hel_I_7 (WP_027065146), 64% similarity with *Eudoraea adriatica* (WP_019670332) and *Emticicia oligotrophica* (WP_015030002) and 63% similarity with *Runella limosa* (WP_028524560) and *Algoriphagus mannitolivorans* (WP_026951097). Sequence alignment shows the conserved motif is Gly 219-X-Ser 221-X-Gly 223 and the catalytic triads are Ser 221-Glu 337-His 456. The multiple sequence alignments of EstH sequence with various closely related genera is shown in Fig. 1.

3.2. Expression and purification of EstH

EstH was expressed and purified in soluble form using *E. coli* BL21 (DE3) cells with the recombinant plasmid pGEX-6P-1-EstH. The recombinant fusion protein (EstH+ GST) had a molecular weight of 87.2 kDa, with 61.2 kDa and 26 kDa for EstH and GST tag, respectively (Fig. 2). The purified EstH was of 61.2 kDa in size with a single band after the removal of GST tag.

3.3. Synthesis and characterization of Fe_3O_4~cellulose nano-composite

The Fe_3O_4 nanoparticles were characterized by Transmission Electron Microscopy (TEM) and the size of each particle ranged from 2 to 20 nm. The diameter of cellulose nanospheres was in the range of 50–200 nm. The sol-gel reaction resulted in the formation of a firm sheath of cellulose around the Fe_3O_4 nanoparticle. The resulting micro-particles showed a larger size as compared to both of these nanostructures (Fig. 3). The O-H and C-H stretching peaks were observed at 2900 cm^{-1} and 2850 cm^{-1} respectively. The bending vibration and deformation vibration of O—H and C—H bonds of cellulose were recorded at 1371 cm^{-1} and 897 cm^{-1}. The peaks at 2800 cm^{-1} and 2900 cm^{-1} showed the stretching vibrations of O—H and C—H, respectively. The major bands at 1430 cm^{-1} were attributed to the C—H deformation vibrations of CH_2 group in cellulose [41]. The bands at 1060 cm^{-1} in the spectra of nano-cellulose were associated with the C—O stretching vibration. The anomeric carbon of cellulose showed the absorption band at 895 cm^{-1}, for NCC. The bands at 588 and 582 cm^{-1} in the spectra of MNPs were the characteristic absorption of the Fe—O bond, confirming the presence of magnetite nanoparticles (Table 1). Although in a previous study of Fe_2O_3 nanoparticles were also represented the Fe—O stretching at 535 cm^{-1} in another study [42].

3.4. Immobilization of purified esterase onto Fe_3O_4~cellulose nano-composite

The purified esterase, EstH was immobilized by incubating the protein with nano-composite for 12 h and separated by using

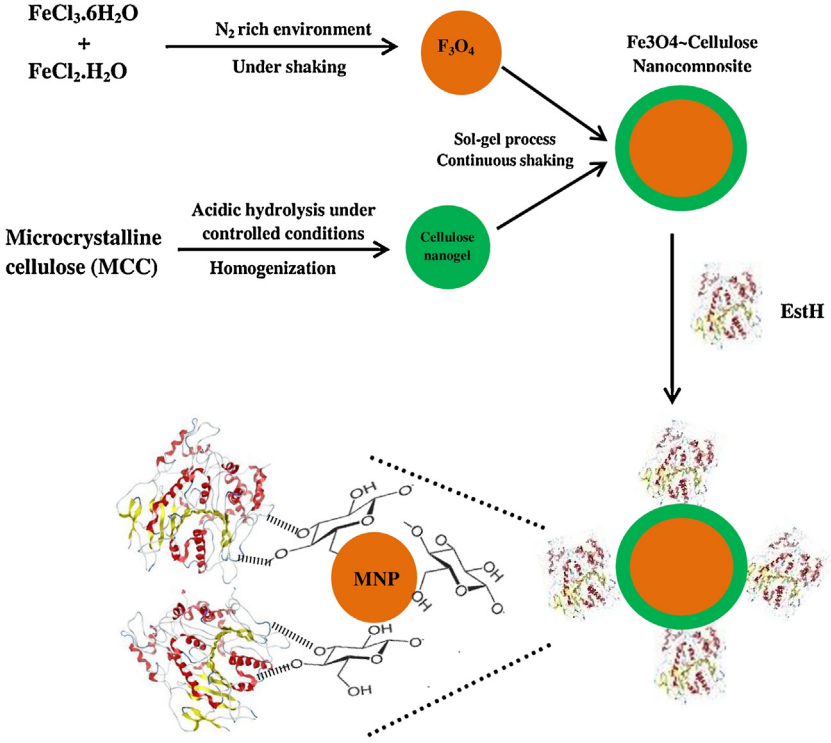

Fig. 4. Schematic representation of immobilization of EstH onto nanocomposites. Schematic representation of nanocomposite synthesis and immobilization of EstH onto that.

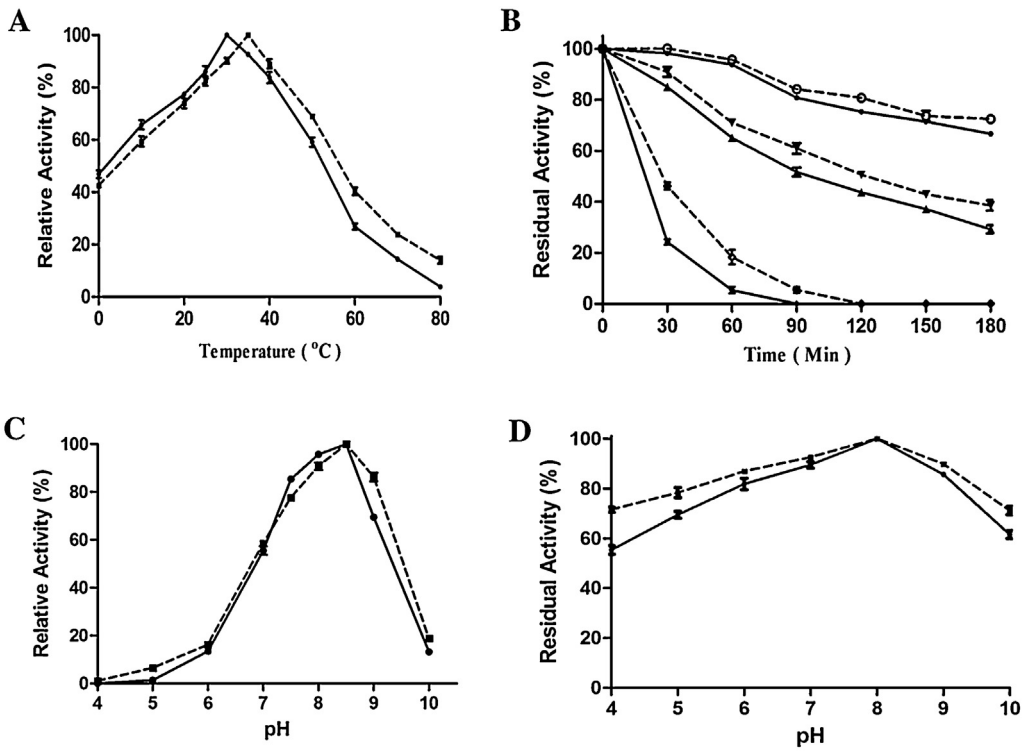

Fig. 6. Effect of temperature and pH on EstH activity and stability. (A) Temperature specificity was investigated by incubating the reaction in a temperature range from 0 to 80 °C (Filled circle for EstH and dotted square for immobilized EstH). The specific activity for EstH at 30 °C and immobilized EstH at 35 °C was defined as 100%. (B) Temperature stability was measured by incubating the enzyme at different temperatures (40 °C, filled circle EstH; dotted empty circle immobilized EstH; 45 °C, filled triangle EstH; inverted dotted filled triangle immobilized EstH; 50 °C empty diamond EstH and dotted filled diamond immobilized EstH). The residual activity was measured at standard conditions and samples were withdrawn every 30 min for 3 h. The specific activity without incubation was defined as 100%. (C) For pH activity test phosphate–citrate buffer (pH 4.0–8.0) and Tris–HCl buffer (pH 8.0–10.0) were used and (D) pH stability was determined under standard conditions by calculating the residual activity after incubating the enzyme for 24 h at 4 °C in the phosphate–citrate buffer (pH 4.0–8.0) and Tris–HCl buffer (pH 8.0–10.0). The activity at pH 8.5 and stability at pH 8 were considered as 100% (Filled circle for EstH and dotted square for immobilized EstH).

magnet on the wall of calibrated tube. The immobilized biocatalyst IY of ~60% binding of the total protein and IE was calculated to be ~75% and enzyme loading was ~10 mg of protein g^{-1} of matrix. The immobilized biocatalyst was washed 3 times with PBS and stored at 4 °C for later use (Fig. 4).

3.5. Comparison of catalytic properties of free and immobilized EstH

Both forms of EstH can hydrolyze short chain esters from C2 to C8, showing the highest activity against C4 and no activity against C12 and C16, indicating that it is an esterase rather than lipase. Free EstH showed 31%, 49% and 22% of relative activity against C2, C6 and C8, which was 23%, 60% and 12% for the immobilized one (Fig. 5). Free EstH showed highest activity at 30 °C with ~50% of relative activity at 0 °C and maintained more than 87% activity from 20 to 40 °C whereas immobilized EstH had the apparent optimal activity at 35 °C with 43% of relative activity at 0 °C and retained more than 92% activity from 20 to 40 °C (Fig. 6A). With gradual increase of temperature and time, the activities of both free and immobilized EstH declined steadily, but varied from each other. After 3 h of incubation, free EstH lost almost 35% activity at 40 °C, but at 50 °C, it showed only 22.40% activity after 30 min of incubation and completely deactivated after 90 min of incubation. However, immobilized EstH lost only 26% activity at 40 °C, and at 50 °C, it showed 48.5% activity after 30 min of incubation and completely deactivated after 120 min of incubation (Fig. 6B). Both forms of EstH presented their maximum activity at around pH 8.5 and were active in a broad pH range (Fig. 6C). After 24 h incubation in different pH buffers, they showed good stability from pH 4–10, with the highest stability at pH 8, and immobilized EstH showed noticeably higher stability compared to the free form. At pH 4 and 10, free EstH showed ~58% and ~63% activity, which was ~73% that of the immobilized one (Fig. 6D).

The stability of free and immobilized EstH against different organic solvents was tested in different concentrations (10–40%, v/v) by incubating them for 40 min. Free EstH showed more than 90% of the original activity in the presence of 10–30%, v/v DMSO and ethanol. However, the activity was greatly reduced by acetonitrile in 20%, v/v concentration and no activity was detected in 30%, v/v. Interestingly in the presence of Ethylene glycol in all tested

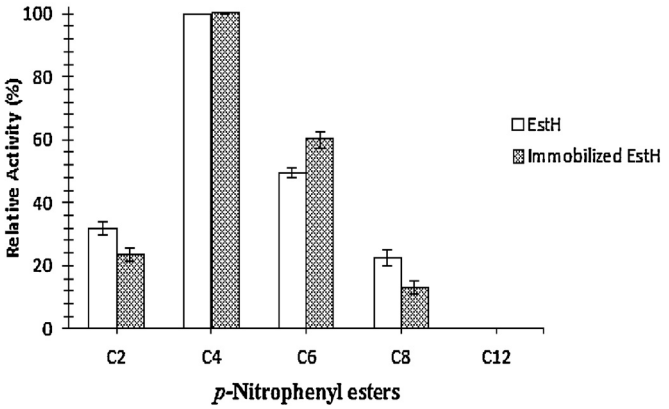

Fig. 5. Substrate specificity of EstH using p-NP esters. Substrate specificity was measured using p-NP esters from C2 to C16. For both free and immobilized EstH, activity towards *p*-nitrophenyl butyrate (C4) was defined as 100%.

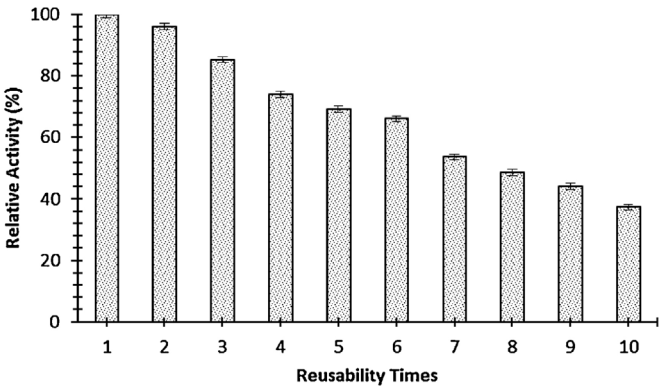

Fig. 7. Measurement of EstH reusability. Reusability was tested by collecting the nano-composite after centrifugation and using it again in the reaction system up to 10 cycles. The reaction was done in standard system and the initial activity was considered as 100%.

concentrations the activity of the immobilized EstH was found to be increased as compared to free one but little or no activity was detected in the presence of 40%, v/v acetonitrile, ethanol and isopropanol (Table 2).

Enzyme recyclability is an important factor for cost reduction in industrial processes. EstH could maintain ~70% of its initial activity after 5 repetitive cycles and ~40% activity after 10 repetitive cycles (Fig. 7). The storage stability of both EstH was determined from 5 days to 50 days in standrad conditions. The immobilized EstH decreased its activity much more slowly compared to the free one, retaining ~ 71% of the initial activity after 50 days of storage at 4 °C versus ~40% activity for the free one (Fig. 8). The 50% decrease in the original activity was reported after 32 h for the Immobilized EstH compared to 18 h for its free form.

Free EstH was inactivated completely when incubated for 1 h at different concentrations of ionic detergents CTAB and SDS, but was slightly stimulated by 0.5% (v/v) non-ionic detergent Tween 20, and remained quite stable even in 1% and 2% (v/v) Tween 20. Additionally, it was obviously inhibited by Tween 80 and Triton X-100, retaining 37.6% and 9.1% activity respectively. In contrast, immobilized EstH remained quite stable in detergents, maintaining 101.2%, 22.1% and 14.1% activity in 2% (v/v) non-ionic detergent Tween 20, Tween 80 and Triton X-100 (Table 3).

Noticeably, both free and immobilized EstH showed a steady increase of activity up to 3 M NaCl and a decrease at 4.5 M NaCl. In the presence of 3 M NaCl, free and immobilized EstH showed 129% and 115% of the original activity, respectively. EstH revealed even high activity when incubated with 1 M to 4.5 M NaCl for 12 h. Free EstH showed 105% activity at 3 M and 89% activity at 4.5 M NaCl whereas immobilized EstH showed 104% and 68% activity at 3 M and 4.5 M NaCl, respectively (Fig. 9). The K_m and K_{cat} values for immobilized EstH were 0.22 mM and 520 s^{-1} versus 0.18 mM and 365 s^{-1} for the free one. Similarly, in a previous study, a-Chymotrypsin immobilized in Polystyrene nanoparticles was reported with increased K_{cat} as compared to free enzyme [43]. Also the *K*m and *V*max of immobilized one were found to be higher than free enzyme has also been reported [44–46].

4. Discussion

Marine environment is a vast pool of novel biocatalysts and more research efforts are being made to identify new genes with unusual properties from marine environment compared to the terrestrial microorganisms [10]. With the gradual development of science and technology, in silico-based search for novel genes from the genomic information available has become an efficient way to clone and characterize industrially important novel enzymes [47]. In this study, a new esterase gene, EstH was cloned from the genomic information of the marine bacterium *Zunongwangia* sp. and the esterase was found to be cold-active and salt-tolerant and was able to improve catalytic properties when immobilized on Fe_3O_4~cellulose nano-composite. Generally, lipases/esterases are basically divided into eight groups according to their amino acid sequences and basic biological properties [35]. Phylogenetic analysis indicates that EstH and its related proteins belong to group VII (Fig. S1). In recent years, some other esterases of this group has been identified and characterized, such as estCS2 from a compost metagenomic library [48], est-XG2 from an activated sludge sample metagenomic library [49] and *est*DL30 from an alluvial soil metagenomic library [50].

Marine microorganisms could be a good source of cold active enzymes [51]. Retaining activity at a low temperature and losing activity at a moderate temperature are the major characteristics of cold active enzymes [52]. EstH showed ~50% of its original activity at 0 °C with the optimal activity at 30 °C and lost its activity quickly at above 50 °C. Low energy consumption to promote the reaction is the most attractive property of the cold active enzymes [53]. Additionally, this type of esterase could be applied to produce frail compounds in an industrial scale [51], quicken inactivation to reduce unexpected chemical reactions and transform heat labile substrates [54], synthesize fragile pharmaceutical compounds and bioremediate waste products in cold conditions [51,55]. Due to the good activity at low temperature, EstH has potential for various industrial applications and bioremediations. The optimal temperature of EstH is the same with some previously reported cold active enzymes [56–59]. At 0 °C, EstH shows almost the same activity with est10 (55%) from *Psychrobacter pacificensis* [52] and estO (50%) from *Pseudoalteromonas arctica* [60]. Interestingly, the optimal temperature of the immobilized EstH shifted from 30 °C to 35 °C. After immobilization, increased thermostability [12,15,16,61,62],

Table 2
Effect of different organic solvent on the stability of EstH.

Compounds	Relative Activity (%)							
	Free Enzyme				Immobilized Enzyme			
	10% (v/v)	20% (v/v)	30% (v/v)	40% (v/v)	10% (v/v)	20% (v/v)	30% (v/v)	40% (v/v)
None	100.0	100.0	100.0	100.0	100.0	100.0	100.0	100.0
Ethylene Glycol	94.0 ± 1.7	82.2 ± 1.2	73.8 ± 1.8	40.4 ± 3.9	113.2 ± 1.2	111.7 ± 1.6	100.5 ± 3.4	55.9 ± 0.2
Acetonitrile	101.1 ± 3.2	21.6 ± 3.1	ND	ND	100.0 ± 2.1	34.5 ± 2.1	ND	ND
Methanol	103.5 ± 0.6	102.3 ± 2.2	80.0 ± 3.2	19.6 ± 1.3	95.6 ± 1.5	72.8 ± 0.7	66.5 ± 3.3	53.7 ± 1.5
DMSO	100.7 ± 0.3	100.4 ± 0.6	91.7 ± 2.3	83.3 ± 2.2	65.8 ± 0.5	72.3 ± 2.2	63.9 ± 1.6	30.4 ± 1.1
Ethanol	104.0 ± 1.0	84.9 ± 2.6	99.6 ± 1.3	40.9 ± 0.8	116.9 ± 4.2	80.7 ± 0.8	15.0 ± 2.1	6.5 ± 1.8
Isopropanol	80.3 ± 2.9	71.7 ± 1.0	66.1 ± 2.7	23.8 ± 1.9	75.7 ± 1.6	37.6 ± 1.8	26.9 ± 0.2	ND

Effects of organic solvents 5–50% (v/v) were tested by incubating the enzyme at room temperature for 40 min. Then the residual activity was determined against that not incubated with any organic solvent under standard conditions. The esterase activity without any additives was defined as 100%. All determinations were performed in triplicate.

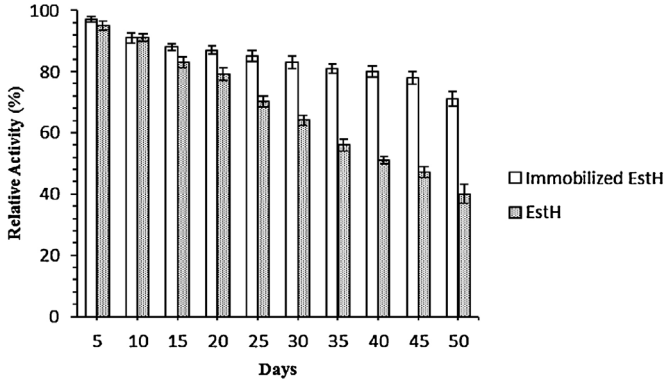

Fig. 8. Determination of the storage stability of EstH. The storage stability of both EstH was determined at a regular interval of five days for fifty days under standrad conditions. The initial activity on the first day was considered as 100%.

and changed optimal temperature such as the increase from 40 °C to 45 °C in the *para*-nitrobenzyl esterase of *Bacillus subtilis* after immobilization in magnetic beads [63], from 30 °C to 37 °C by covalent immobilization of a lipase in carboxyl-activated magnetic nanoparticles [64], from 40 °C to 45 °C in Celite-Immobilized *Candida rugosa* lipase, [65], and from 65 °C to 70 °C after the entrapment of esterase into silicate coated Ca-alginate beads [62] has been reported in various studies. Additionaly, the optimal pH of both free and immobilized EstH was 8.5, which was the same with another cold-adapted esterase, rEstKp from *Pseudomonas mandelii* immobilized on graphene oxide [12]. According to previous reports, the molecular mechanism underlying the cold activity is that the esterase has more glycine and proline residues, less arginine residues and lower proportion of Arg/(Arg + Lys) to give the protein flexibility and plasticity, rendering the enzyme cold active [5,51,53]. In EstH, the ratio of Arg/(Arg + Lys) was only 0.23, much lower than that of the other reported cold adapted esterases [52,66,67], which may be the molecular reason of its cold active property. EstH also showed slightly higher thermostability than some other reported cold active esterases which tend to be inactivated at above 40 °C within a very short time [58,67–69]. To synthesize a thermally and operationally stable enzyme, immobilization on a solid support is an important tool in biotechnology [70], and is the most frequently used method to increase the stability of some enzymes, because immobilization matrix protects the enzyme from being denatured and restricts the conformational change. More interestingly, immobilized EstH displayed better catalytic efficiency at elevated temperatures than the free EstH. At over 60 °C, EstH lost its activity totally, probably due to the disturbance of globular structure of the protein, causing protein unfolding and loss of enzymatic activity. Actually, immobilization gives rigidity through attachment of the enzyme to the matrix, thus preventing protein aggregation and proteolysis like intermolecular process [71]. At high temperature, free EstH was denatured more quickly than the immobilized one. For both the free and immobilized EstH enzymes, heat could make them conformationally flexible but the immobilized one could still be catalytically active [72]. Thus, the thermostability achieved by immobilizing EstH on Fe_3O_4~cellulose nano-composite is useful for industrial applications. Another noteworthy characteristic of EstH is its salt tolerance. EstH is active in the presence of high concentration of NaCl and even works well without the presence of NaCl, indicating that EstH is halotolerant but not halophilic. EstH showed 90% activity after treatment with 4.5 M NaCl. Though immobilization has lessened the salt tolerance slightly, the result is still impressive. After immobilization, EstH showed about 70% activity at 4.5 M NaCl. Generally, halophilic and halotolerant enzymes contain more acidic amino acid residues as a shield to protect the surface of the protein from being dehydrated, or in other words, keep it hydrated by binding with salt ions to minimize the hydrophobicity of the protein and its properties of being aggregated with high salt concentrations [73–75]. EstH contains a large amount of acidic amino acid residues (31 Asp+ 48 Glu; 14.25%), which may impart it salt tolerance, but it needs to be further elucidated in the future. The structural modeling by Molecular Operating Environment (MOE) also reveals the presence of negative surface charge, which may contribute to salt tolerance (Fig. S2). As both free and immobilized EstH enzymes showed, to a certain degree, the tolerance of salt and some organic solvents, it can be used in reactions containing both organic and inorganic media [9].

Enzyme immobilization is a solution to reduce process cost through its reusability [76]. After the 8th cycle, the immobilized EstH retained ~50% of activity, indicating its good industrial potential in reusability efficiency. A lipase from *C. rugosa* was immobilized onto a Eupergit C support and retained only 30% of activity after 5 cycles of reuse [18]; the molecular sieve-immobilized lipase from *Bacillus coagulans* had 58.5% activity after the 5th time of usage [70]. Additionally, storage stability of a biocatalyst is an important factor for the industrial usage. A free enzyme gradually loses its activity during storage, but an immobilized enzyme can show a good storage stability [14,62]. In the present study, EstH showed better storage stability (~71% after 50 days) than the *C. rugosa* lipase immobilized on poly macroporous polymer particles, which showed 50% activity after 54 days of storage at 4 °C [19].

5. Conclusions

In this study, we immobilized a novel cold active and salt tolerant esterase, EstH on Fe3O4~cellulose nano-composite and extensively characterized both the free and immobilized EstH in terms of pH, temperature, relative stability, reusability and storage stability. The results show that a type of immobilization method by covalent attachment enhanced thermostability with a shift of optimal temperature (from 30 to 35 °C), storage stability (~71%

Table 3
Effect of different detergents on EstH.

Detergents	Relative Activity (%)					
	Free Enzyme			Immobilized Enzyme		
	0.5% (v/v)	1%(v/v)	2%(v/v)	0.5%(v/v)	1%(v/v)	2%(v/v)
None	100.0	100.0	100.0	100.0	100.0	100.0
Tween 20	108.3 ± 2.3	100.1 ± 1.0	95.3 ± 1.0	132.8 ± 3.2	113.8 ± 4.3	101.2 ± 4.1
Tween 80	73.6 ± 3.5	57.0 ± 3.2	37.6 ± 2.5	64.8 ± 1.1	43.4 ± 1.8	22.1 ± 1.3
Triton-X-100	40.5 ± 1.7	18.9 ± 1.1	9.1 ± 0.3	41.1 ± 1.9	28.4 ± 1.4	14.1 ± 1.6
SDS (w/v)	ND	ND	ND	6.4 ± 0.8	1.6 ± 0.1	ND
CTAB (w/v)	ND	ND	ND	4.5 ± 0.3	2.1 ± 0.5	ND

Data are presented as mean values ±SD. The enzyme was pre-incubated with different concentrations of detergents for 1 h at room temperature (RT). The residual activity was measured at standard conditions. The esterase activity without any detergents was defined as 100%. All determinations were performed in triplicate. (ND = Not determined).

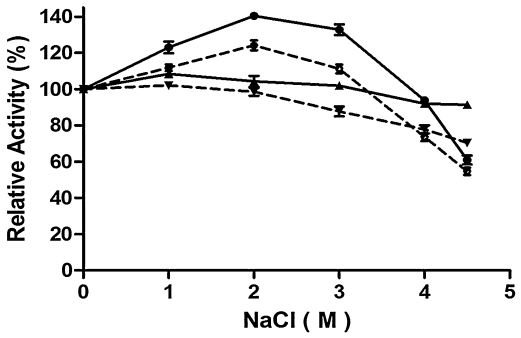

Fig. 9. Effect of NaCl on the activity and stability of EstH. Effect of NaCl on the activity is indicated by filled circle for EstH and dotted square for immobilized EstH and activity was measured at pH 8.5 Tris-HCl (50 mM) buffer with a different concentration of NaCl (0–4.5 M) under the standard conditions. The specific activity without NaCl was defined as 100%. Stability (filled triangle for EstH and inverted dotted filled triangle for immobilized EstH) was determined by incubating the enzyme in pH 8.5 Tris-HCl (50 mM) buffer with different concentrations of NaCl at 4 °C for 12 h, and the relative activity was determined under the standard conditions. The specific activity after incubation with 0 M NaCl was defined as 100%.

activity after 50 days of storage), pH tolerance (pH 4–10) and more importantly, reusability(∼50% activity after 8 cycles of reuse). These newly characterized features of the immobilized EstH suggest that immobilization by covalent bonding can increase the biotechnological potential of this biocatalyst for applications in a wide variety of fields.

Competing interests

The authors claim that they have been no competing interests.

Acknowledgements

This work was supported by grants from National Natural Science Foundation of China (no. 31200580), Hubei province Science and Technology support project (2014BBB009) China, National Science Foundation of China (No. 31270162) and a Project Funded by the Priority Academic Program Development of Jiangsu Higher Education Institutions.

References

[1] T. Panda, B.S. Gowrishankar, Appl. Microbiol. Biotechnol. 67 (2005) 160–169.
[2] F. Hasan, A.A. Shah, A. Hameed, Enzyme Microb. Technol. 39 (2006) 235–251.
[3] U.T. Bornscheuer, FEMS Microbiol. Rev. 26 (2002) 73–81.
[4] U.T. Bornscheuer, C. Bessler, R. Srinivas, S. Hari Krishna, Trends Biotechnol. 20 (2002) 433–437.
[5] R. Cavicchioli, K.S. Siddiqui, D. Andrews, K.R. Sowers, Curr. Opin. Biotechnol. 13 (2002) 253–261.
[6] C. Gerday, M. Aittaleb, M. Bentahir, J.P. Chessa, P. Claverie, T. Collins, S. D'Amico, J. Dumont, G. Garsoux, D. Georlette, A. Hoyoux, T. Lonhienne, M.A. Meuwis, G. Feller, Trends Biotechnol. 18 (2000) 103–107.
[7] R. Margesin, F. Schinner, J. Biotechnol. 33 (1994) 1–14.
[8] A. Oren, FEMS Microbiol. Ecol. 39 (2002) 1–7.
[9] G.A. Sellek, J.B. Chaudhuri, Enzyme Microb. Technol. 25 (1999) 471–482.
[10] X. Jiang, Y. Huo, H. Cheng, X. Zhang, X. Zhu, M. Wu, Extremophiles 16 (2012) 427–435.
[11] M. Matsumoto, K. Ohashi, Biochem. Eng. J. 14 (2003) 75–77.
[12] H.J. Lee, H.K. Han, J. Chung, H.-S. Jang, S.-H. Lee, C. Woo, Bioresour. Technol. 148 (2013) 620–623.
[13] G. Feller, J. Phys. Condens. Matter. 22 (2010) 0953–8984.
[14] A. Yahşi, F. Şahin, G. Demirel, H. Tümtürk, Int. J. Biol. Macromol. 36 (2005) 253–258.
[15] Rodrigo Volcan Almeida, Roberta Vieira Branco, Bruno Peixoto, Cíntia da Silva Lima, Sylvia Maria Campbell Alqueres, Orlando Bonifácio Martins, Octavio Augusto Ceva Antunes, Denise Maria Guimarães Freire, Biochem. Eng. J. 39 (2008) 531–537.
[16] R.V. Branco, M.L.E. Gutarra, J.M. Guisan, D.M.G. Freire, R.V. Almeida, J.M. Palomo, BioMed Res. Int. 2015 (2015) 250532.
[17] P. Villeneuve, J.M. Muderhwa, J. Graille, M.J. Haas, J. Mol. Catal. B: Enzym. 9 (2000) 113–148.
[18] Z. Knezevic, N. Milosavic, D. Bezbradica, Z. Jakovljevic, R. Prodanovic, Biochem. Eng. J. 30 (2006) 269–278.
[19] B.K. Vaidya, G.C. Ingavle, S. Ponrathnam, B.D. Kulkarni, S.N. Nene, Bioresour. Technol. 99 (2008) 3623–3629.
[20] S. Kumar, A. Dwevedi, A.M. Kayastha, J. Mol. Catal. B: Enzym. 58 (2009) 138–145.
[21] D. Bozhinova, B. Galunsky, G. Yueping, M. Franzreb, R. Köster, V. Kasche, Biotechnol. Lett. 26 (2004) 343–350.
[22] P. Blanco, M. Fernández-Pérez, C. Otero, G. Díaz-González, J. Mol. Catal. B: Enzym. 30 (2004) 83–93.
[23] C. Sun, J.S.H. Lee, M. Zhang, Adv. Drug Deliv. Rev. 60 (2008) 1252–1265.
[24] S. Laurent, D. Forge, M. Port, A. Roch, C. Robic, L. Vander Elst, R.N. Muller, Chem. Rev. 108 (2008) 2064–2110.
[25] P.Z. Xu, G.M. Huang, D.L. Feng, C.L. Hu, S. Zhao, M.H. Lai, C. Wei, Z. Huang, C. Xie, G.X. Liu, Z. Feng, Sci. Total Environ. 424 (2012) 1–10.
[26] J. Xu, J. Sun, Y. Wang, J. Sheng, F. Wang, M. Sun, Molecules 19 (2014) 11465–11486.
[27] D. Klemm, F. Kramer, S. Moritz, T. Lindstrom, M. Ankerfors, D. Gray, A. Dorris, Angew. Chem. Int. Ed. Engl. 50 (2011) 5438–5466.
[28] S. Beck-Candanedo, M. Roman, D.G. Gray, Biomacromolecules 6 (2005) 1048–1054.
[29] A. Maleki, M. Kamalzare, Catal. Commun. 53 (2014) 67–71.
[30] S. Liu, X. Luo, J. Zhou, Magnetic responsive cellulose nanocomposites and their applications, in: T.G.M. van de Ven (Ed.), Cellulose–Medical, Pharmaceutical and Electronic Applications, InTech, Rijeka, Croatia, 2013, pp. 105–124, chap 6.
[31] A. Ivanova, K. Fominykh, D. Fattakhova-Rohlfing, P. Zeller, M. Doblinger, T. Bein, Inorg. Chem. 54 (2015) 1129–1135.
[32] J. Zhou, R. Li, S. Liu, Q. Li, L. Zhang, L. Zhang, J. Guan, J. Appl. Polym. Sci. 111 (2009) 2477–2484.
[33] Q.L. Qin, X.Y. Zhang, X.M. Wang, G.M. Liu, X.L. Chen, B.B. Xie, H.Y. Dang, B.C. Zhou, J. Yu, Y.Z. Zhang, BMC Genomics 11 (2010) 1471–2164.
[34] M.M. Bradford, Anal. Biochem. 72 (1976) 248–254.
[35] J.L. Arpigny, K.E. Jaeger, Biochem. J. 343 (1999) 177–183.
[36] K. Tamura, G. Stecher, D. Peterson, A. Filipski, S. Kumar, Mol. Biol. Evol. 30 (2013) 2725–2729.
[37] M. Ioelovich, Nanosci. Nanotechnol. 2 (2012) 9–13.
[38] A. Kumar, S. Zhang, G. Wu, C.C. Wu, J. Chen, R. Baskaran, Z. Liu, Colloids Surf. B Biointerfaces 136 (2015) 1042–1050.
[39] H.-M. Jiang, Z.-P. Yan, Y. Zhao, X. Hu, H.-Z. Lian, Talanta 94 (2012) 251–256.
[40] S.K. Patel, V.C. Kalia, J.H. Choi, J.R. Haw, I.W. Kim, J.K. Lee, J. Microbiol. Biotechnol. 24 (2014) 639–647.
[41] M.M.F.A. Ibrahim Agblevor, W.K. El-Zawawy, BioResources 5 (2010) 397–418.
[42] S.K.S. Patel, S.H. Choi, Y.C. Kang, J.-K. Lee, Nanoscale (2016) http://pubs.rsc.org/en/content/articlepdf/2016/nr/c6nr00346j.
[43] H. Jia, G. Zhu, P. Wang, Biotechnol. Bioeng. 84 (2003) 406–414.
[44] R.O. Cristovao, S.C. Silverio, A.P. Tavares, A.I. Brigida, J.M. Loureiro, R.A. Boaventura, E.A. Macedo, M.A. Coelho, World J. Microbiol. Biotechnol. 28 (2012) 2827–2838.
[45] B. Sahoo, S.K. Sahu, D. Bhattacharya, D. Dhara, P. Pramanik, Colloids Surf. B Biointerfaces 101 (2013) 280–289.
[46] T.N. Nwagu, B.N. Okolo, H. Aoyagi, World J. Microbiol. Biotechnol. 28 (2012) 335–345.
[47] H. Kwoun Kim, Y.J. Jung, W.C. Choi, H.S. Ryu, T.K. Oh, J.K. Lee, FEMS Microbiol. Lett. 235 (2004) 349–355.
[48] C.-H. Kang, K.-H. Oh, M.-H. Lee, T.-K. Oh, B.H. Kim, J.-H. Yoon, Microb. Cell Fact. 10 (2011) 41.
[49] H. Shao, L. Xu, Y. Yan, J. Ind. Microbiol. Biotechnol. 40 (2013) 1211–1222.
[50] W. Tao, M. Lee, J. Wu, N. Kim, S.-W. Lee, J. Microbiol. 49 (2011) 178–185.
[51] B. Joseph, P.W. Ramteke, G. Thomas, Biotechnol. Adv. 26 (2008) 457–470.
[52] G. Wu, G. Wu, T. Zhan, Z. Shao, Z. Liu, Extremophiles 17 (2013) 809–819.
[53] G. Feller, C. Gerday, Nat. Rev. Microbiol. 1 (2003) 200–208.
[54] J. Jeon, J.-T. Kim, S. Kang, J.-H. Lee, S.-J. Kim, Mar. Biotechnol. 11 (2009) 307–316.
[55] K. Novototskaya-Vlasova, S. Yakimov, L. Petrovskaya, D. Gilichinsky, FEMS Microbiol. Ecol. 82 (2012) 367–375.
[56] M.H. Lee, K.S. Hong, S. Malhotra, J.H. Park, E.C. Hwang, H.K. Choi, Y.S. Kim, W. Tao, S.W. Lee, Appl. Microbiol. Biotechnol. 88 (2010) 1125–1134.
[57] L. Kulakova, A. Galkin, T. Nakayama, T. Nishino, N. Esaki, Biochim. Biophys. Acta (BBA)—Proteins Proteomics 1696 (2004) 59–65.
[58] E.Y. Yu, M.A. Kwon, M. Lee, J.Y. Oh, J.E. Choi, J.Y. Lee, B.K. Song, D.H. Hahm, J.K. Song, Appl. Microbiol. Biotechnol. 90 (2011) 573–581.
[59] P. Mander, S. Cho, J. Simkhada, Y. Choi, D. Park, J. Ha, J. Yoo, Biotechnol. Bioproc. E. 17 (2012) 67–75.
[60] R. Al Khudary, R. Venkatachalam, M. Katzer, S. Elleuche, G. Antranikian, Extremophiles 14 (2010) 273–285.
[61] S. Montero, M.D. Virto, D. María, C. Landeta, I. Agud, R. Solozabal, J.M. Lascaray, M. Renobales, M.J. Llama, J.L. Serra, Enzyme Microb. Technol. 15 (1993) 239–247.
[62] S. Gülay, G. Şanlı-Mohamed, Int. J. Biol. Macromol. 50 (2012) 545–551.
[63] J.-M. Park, M. Kim, J.-Y. Park, D.-H. Lee, K.-H. Lee, J. Min, Y.-H. Kim, Process Biochem. 45 (2010) 259–263.
[64] Y.T. Zhu, X.Y. Ren, Y.M. Liu, Y. Wei, L.S. Qing, X. Liao, Mater. Sci. Eng. C Mater. Biol. Appl. 38 (2014) 278–285.
[65] S. Fadıloğlu, Z. Söylemez, J. Agric. Food Chem. 46 (1998) 3411–3414.
[66] G. Wu, S. Zhang, H. Zhang, S. Zhang, Z. Liu, J. Mol. Catal. B: Enzym. 98 (2013) 119–126.

[67] J. Fu, H.K. Leiros, D. de Pascale, K.A. Johnson, H.M. Blencke, B. Landfald, Appl. Microbiol. Biotechnol. 97 (2013) 3965–3978.
[68] H. Cieśliński, A.M. Białkowska, A. Długołecka, M. Daroch, K.L. Tkaczuk, H. Kalinowska, J. Kur, M. Turkiewicz, Arch. Microbiol. 188 (2007) 27–36.
[69] K.-C. Ko, S.-O. Rim, Y. Han, B. Shin, G.-J. Kim, J. Choi, J. Song, J. Ind. Microbiol. Biotechnol. 39 (2012) 681–689.
[70] S. Raghuvanshi, R. Gupta, J. Ind. Microbiol. Biotechnol. 36 (2009) 401–407.
[71] M. Basri, W.M.Z.W. Yunus, W.S. Yoong, K. Ampon, C.N.A. Razak, A.B. Salleh, J. Chem. Technol. Biotechnol. 66 (1996) 169–173.
[72] M.B. Abdul Rahman, S.M. Tajudin, M.Z. Hussein, R.N.Z.R. Abdul Rahman, A.B. Salleh, M. Basri, Appl. Clay Sci. 29 (2005) 111–116.
[73] S. Fukuchi, K. Yoshimune, M. Wakayama, M. Moriguchi, K. Nishikawa, J. Mol. Biol. 327 (2003) 347–357.
[74] M. Müller-Santos, E.M. de Souza, O. Pedrosa Fde, D.A. Mitchell, S. Longhi, F. Carrière, S. Canaan, N. Krieger, Biochim. Biophys. Acta 8 (2009) 719–729.
[75] J. Gomes, W. Steiner, Food Technol. Biotechnol. 42 (2004) 223–235.
[76] A. Chaubey, R. Parshad, S. Koul, S. Taneja, G. Qazi, Appl. Microbiol. Biotechnol. 73 (2006) 598–606.